

Early BHs: simulations and observations

Nico Cappelluti^{1,2,3,4}, Tiziana Di-Matteo⁵, Kevin Schawinski⁶ and Tassos Fragos⁷

¹INAF - Osservatorio Astronomico di Bologna, via Ranzani 1, 40127, Bologna, Italy
email: nico.cappelluti@oabo.inaf.it

²Department of Physics, Yale University, P.O. Box 208121, New Haven, CT 06520, USA, ³Yale Center for Astronomy & Astrophysics, Physics Department, P.O. Box 208120, New Haven, CT 06520, USA, ⁴University of Maryland, Baltimore County, 1000 Hilltop Circle, Baltimore, MD 21250, USA, ⁵McWilliams Center for Cosmology, Carnegie Mellon University, 5000 Forbes Avenue, Pittsburgh, PA 15213, USA, ⁶Institute for Astronomy, Department of Physics, ETH Zurich, Wolfgang-Pauli-Strasse 27, CH-8093 Zurich, Switzerland, ⁷Geneva Observatory, University of Geneva, Chemin des Maillettes 51, 1290 Sauverny, Switzerland

Abstract. We report recent investigations in the field of Early Black Holes. We summarize recent theoretical and observational efforts to understand how Black Holes formed and eventually evolved into Super Massive Black Holes at high- z . This paper makes use of state of the art computer simulations and multiwavelength surveys. Although non conclusive, we present results and hypothesis that pose exciting challenges to modern astrophysics and to future facilities.

Keywords. galaxies: active, galaxies: high-redshift, (cosmology:) early universe

1. Introduction

The mechanism that leads to the formation of a Supermassive Black Holes is still a matter of debate and can be considered one of the unresolved mystery of modern astrophysics. What we know is that in less than 1 Gyr (i.e. by $z \sim 7$) SMBH were able to grow to masses of the order $\sim 10^{10} M/M_{\odot}$. It is very difficult to explain such a rapid growth with *classic* accretion starting from stellar mass seed Black Holes (BHs). In general, we believe that some physical mechanisms had to produce BH seeds with masses in the range 10^2 - $10^5 M/M_{\odot}$. However BHs in such a mass range have been seldom observed in the local Universe therefore, the formation of such BHs could have happened likely only in the early Universe. But also this wisdom has been challenged recently. The peculiar metallicity condition of the early Universe made possible the formation of very massive stars which could rapidly collapse into massive BHs. Under specific circumstances, it has been proposed the direct collapse of pristine, giant molecular clouds into massive $\sim 10^5 M/M_{\odot}$ BHs.

Since no direct detections of these BH seeds was ever achieved, astronomers are undertaking new challenging observations and developing state of the art simulations to understand black holes, galaxies and star formation in general in the Early Universe.

In this paper we present new points of view and developments in the study of early BHs, in Section 2 we present simulations, in Section 3 we discuss signatures of early black holes in cosmic backgrounds and observational challenges, in Section 5 the origin and growth of the first black holes and in Section 6 the evolution of X-ray binaries across cosmic time and energy feedback at high redshift. This paper is meant to be a good summary of the authors presentation at the session on early BHs of the IAU-FM6.

2. Simulations

Numerical simulations of the Universe are now the dominant tool in theoretical cosmology. We have led the development of cosmological codes adapted to Petascale supercomputers and used these resources to understand how supermassive blackholes and galaxies formed, from the smallest to the rarest and most luminous. With nearly one trillion particle we have carried out the BlueTides simulation on BlueWaters. BlueTides is the largest ever simulation with full physics (hydrodynamics, star formation, black holes), and is targeted at the early Universe of galaxies and quasars. The simulation can be compared to cutting edge observations from the Hubble Space telescope, finding good agreement with the properties of observed galaxies when the Universe was only 5 percent of its current age. This simulation actually covers a sky area 300 times larger than the largest current survey with Hubble, allowing us to make predictions for what the upcoming successors to Hubble will see. Scanning through the millions of galaxies that formed in the simulation, we find that large disk galaxies, as massive as the Milky Way as well as the first quasars at $z = 8$. These objects will be exciting targets for the upcoming frontier of observations. Numerical simulations of the Universe are now the dominant tool in theoretical cosmology. Their ability to model the complex physics of structure formation in the Universe is increasing, driven by advances in both computer power and the software algorithms that can use it to full advantage. We need simulations that cover a vast dynamic range of space and time scales and include the effect of gravitational fields that are generated by (dark matter in) superclusters of galaxies upon the formation of galaxies. These galaxies, in turn, harbor gas that cools and makes stars and is being funneled into supermassive black holes that are of the size of the solar system. As this process has entered the petascale regime, it is finally possible with our newly developed MP-Gadget cosmological code to answer questions in cosmology which require simulations of the entire visible universe at high mass and spatial resolution. This applies to making direct predictions for what should be seen in future observations and surveys as well as using the simulation as tools to mock future surveys. The simulations follow the evolution of the matter, energy and radiation in model universes from the Big Bang to the present day. In BlueTides, the actions of gravity, hydrodynamics, forming stars, black holes, molecular gas, inhomogeneous ionizing radiation and more were all included. We have carried out a full-machine run on the NSF NICS high-performance computer Blue Waters, the BlueTides cosmological simulation with MP-Gadget. The simulation aims to understand the formation of the first quasars and galaxies from the smallest to the rarest and most luminous, and The Blue Tides simulation has successfully used the essentially the entire set of XE6 nodes on the Blue Waters machine. It is following the evolution of 0.7 trillion particles in a large volume of the universe (600 co-moving Mpc on a side) over the first billion years of the universes evolution with a dynamic range of 6 (12) orders of magnitude in space (mass). This makes BlueTides by far the largest cosmological hydrodynamic simulation ever run. The Blue Tides run was made possible through a number of improvements applied to the cosmological code Gadget - now MP-Gadget, fully instrumented to run on Petascale resources. MP-Gadget is the the main source code of BlueTides simulation that scales to Petascale and beyond. As BlueTides includes a complicated blend of different physics that is non-linearly coupled on a wide range of scales, which leads to extremely complex dynamics. Without significant investment of effort in code development, including radical improvements in efficiency and load balancing it would have been impossible to carry out the run. Significant efforts were spent in code development and model validation. Some of the major code improvements include: these role of these processes in the reionization of the universe.

- Threading efficiency: We replaced global critical sections with per-particle (per-node) spin locks. The code is now truly scalable to any number of threads. The improved thread-

ing efficiency allows us to use fewer domains, which in turn further reduces the complexity of domain decomposition and inter-domain communication, improving the overall efficiency of the code.

- Mesh gravity solver : Domain decomposition was an issue with the huge Fourier Transforms (up to 163843) needed to carry out the large-scale mesh computation of the gravitational force. We have been able to improve the speed of this part by a factor of 10 (as measured on BlueWaters) by upgrading the Fourier Transform (FT) used to compute the gravitational force from a slab decomposition to a “pencil” decomposition, which allows the computation to be efficiently distributed among the 20,000+ XE6 nodes of Bluewaters.

- MP-sort : We implemented and published with BW staff a new sorting algorithm that exchanges one data item exactly once. ($O[N]$ communication) It worked (200 seconds to build our galaxy catalogs (FOF)), and is only limited by the network bandwidth.

We have also improved the physical modeling in MP-Gadget:

- A new pressure-entropy SPH formulation (Hopkins *et. al*) replaces the old density-entropy formulation, which produces suppresses phases mixing in a non-physical way.

- We incorporate a patchy reionization model from Battaglia *et al.* the model introduces a UV field based on a predicted time-of-reionization at different spatial location in the simulation.

- We have improved stellar feedback models to include mass/halo dependent supernova wind efficiency (similar metal cooling and H2 mass fraction)

The simulation has produced tens of snapshots, 40 TB each of data on particle positions and properties, a total of 2 PB. After refining our own software to deal with these enormous data volumes, we have carried out the following initial analyses. A Giga-Pan terapixel image of the MassiveBlack cosmological simulation which was run for this project is available for this project. *Science Results:* We have used our stellar modeling to compute the visible light distribution in the simulation, and by projecting this with an appropriate kernel, we have made multi-gigapixel maps of the simulation sky as they would be seen by an observer.

- First galaxies: We have applied observational selection algorithms (the widely used SourceExtractor software) to the simulated sky maps and created catalogs of millions of galaxies. Making use of the high resolution of BlueTides we have made detailed images of individual galaxies, uncovering a striking and unexpected population of large Milk Way-sized disk galaxies present when the universe was 5% of its present age (Feng *et al.* 2015).

- First quasars. From our simulated catalogs, we have computed statistical measures of the population of galaxies and quasars at different redshifts, showing consistency with some early data from the Hubble Space telescope, and making predictions for upcoming surveys. We also make predictions for the next frontier of massive black holes that assemble at these early epoch and have masses of 100 million times that of Sun (Feng *et al.* 2016).

- Reionization from galaxies and quasars :Our newBlueTides simulation allows us to study the luminosity functions of the first galaxies and quasars, and their contribution to reionization. We have investigated how these luminosity functions affect the progress of reionization, and find that a high escape fraction is required if galaxies dominate the ionizing photon budget during reionization. With smaller galaxy escape fractions a large contribution from the faint quasars is feasible (Di-Matteo *et al.* 2015, in prep.).

In the coming decade, a new generation of astronomical instruments, all in the billion dollar-class will start making observations of the universe during the period of the first stars and quasars, and opening up the last frontier in astronomy and cosmology. Those that are specifically targeting this epoch as their highest priority include the Square

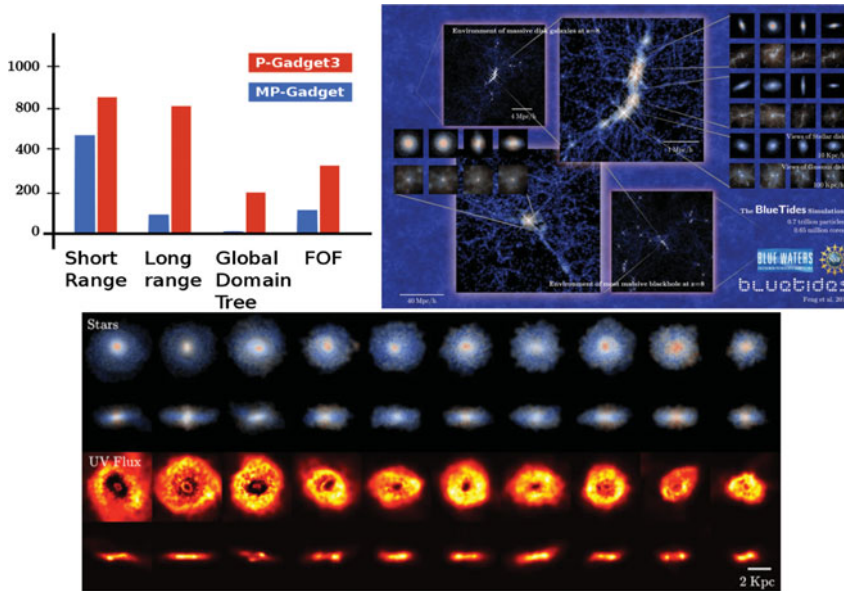


Figure 1. *Top Left Panel* :Comparing the walltime in a single step in MP-Gadget and P-Gadget. in BlueTides simulation. Even with more physics modules, the short-range force in P-Gadget still spends less time per step than P-Gadget3. The long range force module in MP-Gadget out-performs P-Gadgets by a factor of 8. The global domain builder a factor of 10 and the galaxy catalogue (FOF) builder a factor of 2.*Top Right panel*:The large scale gas density fields in projection (top/bottom). The rectangular insets show the formation of Milky-Way mass disk galaxy and the insets at the bottom the most massive black hole when the universe is 5% of its current age. Its host galaxy is much more spheroidal. *Bottom Panel*: The most massive galaxies at $z = 8$ are disky. The top two rows shows the projection of stellar density (face on and edge-on) for a sample of massive galaxies in the BlueTides simulations. The two bottom rows show the corresponding star-formation rate density for the same galaxies.

Kilometer Array radio telescope, the NASA James Webb Space Telescope, the successor to Hubble, and several huge ground-based telescopes, such as the Thirty Meter Telescope, the European Extremely Large Telescope, and the Giant Segmented Meter Telescope, each of which have collecting areas an order of magnitude larger than the current largest scopes.. However, doing observation and experiment without theories to test and models to build understanding will give a very limited return on this investment.

3. Signatures of early black holes in Cosmic Backgrounds and observational challenges.

Cosmological models predict the emergence of the first stars, supernovae and black holes at redshifts $z \sim 30$. The expectation is that in the early Universe there was a mixture of stellar populations: Pop III stars, formed out of still pristine gas, and characterized by an initial mass function (IMF) that is very uncertain, but is thought to be biased towards high masses; and Pop II stars described by a Salpeter-like IMF. In addition to these stellar sources, the production of ionizing photons from accreting black holes (BHs) could possibly play a major role in shaping the high- z IGM (e.g. Mirabel *et al.* 2011). Such BH activity could originate in either the relics of massive Pop III or Pop II stars, or in the direct collapse of primordial gas clouds to $10^5 M_{\odot}$ massive BHs. These black holes can therefore be considered as progenitors of Supermassive BHs (SMBHs) with mass of the order $10^5 M_{\odot}$ observed already at $z \sim 7$, i.e. when the Universe was 0.5 Gyr old (Mortlock *et al.* 2011). On the other hand, constraints from the unresolved X-ray background make it difficult to account for the first generation of supermassive black holes from standard accretion processes (Salvaterra *et al.* 2012). The nature of the progenitors

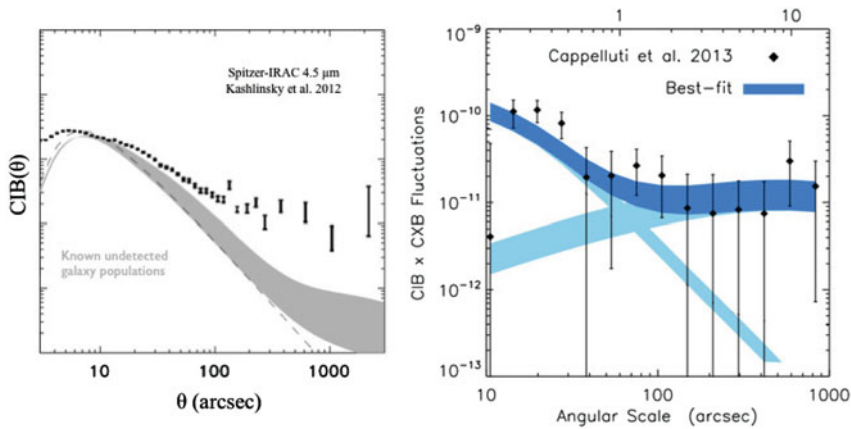


Figure 2. Left: CIB fluctuations at $4.5\ \mu\text{m}$ as measured by Kashlinsky *et al.* (2012) compared with the predicted amplitude of CIB power known galaxy populations from Helgason *et al.* (2012). Right: the cross power spectrum between $4.5\ \mu\text{m}$ and 0.5–2 keV (Spitzer and Chandra) CIB and CXB fluctuations measured by Cappelluti *et al.* (2013) and modeled by Helgason *et al.* (2012) with a foreground known sources component plus a high- z clustering component.

of SMBH is thus one of the most challenging questions of modern astrophysics. Unfortunately, early black hole seeds and first galaxies are inaccessible to current telescopic studies. Nevertheless, the integrated residual background emission contains valuable information about the earliest source populations. The Cosmic Infrared Background (CIB) is the collective radiation emitted throughout cosmic history, including from sources not directly detectable (Kashlinsky *et al.* 2005), and its fluctuation power spectrum carries information on the nature and environment of the primordial sources. The measured spatial power spectrum of the CIB fluctuations rises above the expected contribution from known sources at large scales >20 (Kashlinsky *et al.* 2012). The amplitude and shape of this excess is a direct measurement of the clustering properties of the sources responsible for the fluctuations, and thus a primary key to understanding the nature of these sources. The interpretation of these power spectra has been a matter of debate. However, it is now firmly established that the power spectra are inconsistent with the emission of presently resolved galaxies ($z < 6$) with extrapolation to lower luminosities (Helgason *et al.* 2012). The measurements are consistent with a high-redshift origin, but the largest diagnostic power is at wide angular separations. A detailed comparison with cosmological models has been hitherto impossible because the Spitzer and AKARI fields are limited in size and number, with fluctuations only measured to scales of <0.3 deg and with large uncertainties (see Fig. 2). The unresolved X-ray background also contains information about the earliest source populations. Recently, it has been determined the existence of a significant crosscorrelation between the source-subtracted CIB and cosmic X-ray background (CXB) fluctuations in the AEGIS field (Cappelluti *et al.* 2013); this is illustrated in Fig. 2. The measured cross-power indicates that >15 – 25% of the CIB power is produced by objects associated with sources of powerful X-ray emission. The corresponding CIB is not easily explained with sources in the present-day Universe, but could originate at early epochs where the Universe could have contained very substantial BH populations contributing a large fraction of the CIB signal. Semi-analytical models predict different shapes and amplitudes of the CIB-CXB auto- and cross-power depending on the nature of the sources producing them (i.e. Pop III star remnants, BH seeds powered by the gas envelopes of giant collapsed clouds), but better and more detailed measurements are required to obtain significant constraints. Kashlinsky *et al.* (2007) show that in the GOODS regions observed at both IRAC and the Hubble ACS bands

($0.9 \mu\text{m}$) to $m_{AB} \sim 28$, there are no correlations between the source-subtracted IRAC maps and the same area mapped with ACS. This result may imply that the Lyman break wavelength of the source population responsible for the NIR emission is redshifted beyond the longest ACS wavelength, unless the CIB anisotropies come from more local but extremely faint and so far unobserved galaxies (i.e. $m_{AB} > 28$). This likely requires that the detected CIB fluctuations arise from objects within the first Gyr of the Universe's evolution. The signal is isotropic on the sky, consistent with a cosmological origin, as testified from the CIB spectra in seven different locations on the sky in Kashlinsky *et al.* (2012). The large-scale source subtracted CIB fluctuations are well fit with the prescription of the Λ -CDM model density field at high- z as shown by the blue solid line in Fig. 2; this clustering is very different from that of normal galaxy populations at recent epochs (see Fig. 2). The same results have been reproduced with Akari by Matsumoto *et al.* (2011). The CIB fluctuations are highly correlated on scales larger than 10-20 with the Chandra 0.5-2 keV unresolved CXB. This suggests that at least 20% of the CIB fluctuations are associated with accreting X-ray sources (likely BHs, see e.g. Mirabel *et al.*, 2011). This measurement has been obtained thanks to the excellent performance of Spitzer and Chandra, especially to the negligible instrumental noise of the ACIS-I detector. The study of the joint CXB and CIB fluctuations has been performed on scales $< 13'$ in the AEGIS field where, because of the pattern of the mosaic the largest scales are poorly sampled. The scales around $10'$ - $30'$ are the most interesting to study if we want to firmly establish that these sources are high- z black holes and open a new window on the early Universe. In fact, if the sources responsible for the CXB and CIB fluctuations are at high redshift (i.e. $z > 7-8$) and distributed according to the established Λ -CDM model, their angular CXB/CIB fluctuation spectrum should exhibit a (shallow) peak around $10'$ - $15'$. Yue *et al.* (2013) proposed that a population of highly obscured Direct Collapse Black Holes (DCBH) at $z \sim 12$ could explain the observed level of the 3.6 and $4.5 \mu\text{m}$ fluctuations on scales $> 100''$. On smaller scales the fluctuation are produced by undetected galaxies at low and intermediate redshifts. Albeit Compton-thick, at scales $> 100''$ DCBHs could produce a CXB (0.52 keV)-CIB ($4.5 \mu\text{m}$) cross-correlation signal of $10^{-11} \text{ erg s}^{-1} \text{ cm}^{-2} \text{ nW m}^{-2} \text{ sr}^{-1}$ slightly dependent on the specific value of the absorbing gas column ($N_H \sim 10^{25} \text{ cm}^{-2}$). At smaller scales the cross-correlation is dominated by the emission of high-mass X-ray binaries hosted by the same low- z , undetected galaxies accounting for small-scale NIRB fluctuations. This model opens a very interesting window on the early Universe. On the other hand the high- z interpretation has been challenged by Cooray *et al.* (2012) who explained the shape of the CIB excess as the contribution of the Intra-Halo-Light (IHL) emission from stars stripped during mergers.

While giant BHs have been detected by the SDSS in luminous QSOs (e.g. Mortlock *et al.* 2011), several attempts have been performed to obtain a direct detection of the early stage of accretion onto SMBH seeds. Stacking of X-ray photons at the position of known high- z sources is one of these (e.g. Treister *et al.* 2013) however, like in the case of background fluctuations one could get only an ensemble picture of a population of preselected galaxies and not a direct/individual detection of any of sources. Other techniques use PSF fitting with HST deep catalogs as priors for the source detection (Cappelluti *et al.* 2016, submitted; Fiore *et al.* 2012; Giallongo *et al.* 2015) but results are still controversial and highly debated.

Recent interpretations of the spectra and the environment of bright Ly- α emitters like CR-7 (Sobral *et al.* 2015), suggest these sources could be actually powered by DCHB (Pallottini *et al.* 2015; Agarwal *et al.* 2015). However the smoking gun for such a scenario would be the detection of X-rays from a Ly- α emitter. However, the sensitivity of Chandra is just enough to provide a detection only with a very long exposure. This means that this kind of investigation could be cornerstones of the next generation of X-ray telescopes like Athena or the X-ray surveyor.

4. The origin and growth of the first black holes

Observational constraints of black hole seed formation and early growth models are starting to become possible using ultra-deep X-ray surveys with *Chandra*. The *Chandra* Deep Field South (CDFS) is currently the deepest field available and covers an area of ~ 500 sq. arcmin (Xue *et al.* 2011). The same field also contains the deepest coverage at optical and near-IR wavelengths with *Hubble* and so on the order of several hundred $z > 5$ galaxies have been reported by various groups. If seed formation is common in the early universe, and some fraction of these seed black holes are growing at $5 < z < 10$, then X-ray observations with *Chandra* should be able to detect this growth. At high redshifts, the observed 0.5–10 keV energy band of *Chandra* shifts to the restframe hard X-rays and so even high levels of obscuration, whether nuclear or host galaxy, should have only a moderate effect on detectability.

There are two observational strategies one can employ in locating high redshift AGN: the first is to take all detected X-ray sources in the CDFS and performing a detailed analysis of each source to determine whether it could be at $z > 5$ given the available multiwavelength data. Weigel *et al.* (2015) present such an analysis and conclude that none of the X-ray sources in the overlap region of the CDFS data and the CANDELS data are likely at $z > 5$. The second strategy is to take all reported high redshift *galaxies* and stack their X-ray data. Since the background of *Chandra* is very low, stacking is a highly efficient technique. Treister *et al.* (2013) stack the *Chandra* 4 Msec data of $z \sim 6$, 7 and 80 Lyman Break Galaxies (LBGs) and report non-detections in each redshift bin. The sensitivity limits reached by this analysis would have detected a signal if the typical AGN X-ray luminosity of these LBGs is in the range of $\sim 10^{41-42}$ erg/s.

The complementary null results of Treister *et al.* (2013) and Weigel *et al.* (2015) can be interpreted in a number of ways:

(a) Black hole seed formation efficiency is very low and so most galaxies at $5 < z < 10$ do not yet contain black holes, even though these galaxies are likely to grow to massive galaxies by the present day

(b) LBGs at high redshift contain massive black holes, but they do not accrete. Since LBGs at this redshift are highly star-forming, they must also be gas rich, so why do their central black holes not accrete?

(c) Early massive black holes could be highly obscured so that even restframe hard X-rays fail to locate them, or they could grow via radiatively inefficient accretion (see e.g. Madau *et al.* 2014 and Volonteri *et al.* 2015)

Of course, these various explanations are not mutually exclusive, and the pressure on predictions from simulations (e.g. Treister *et al.* 2013) is not yet significantly constraining. The lack of any evidence for AGN at $z > 5$ in deep surveys, unlike wide-area quasar surveys, is at present not explained. Alternative explanations for seed formation includes scenarios where seed formation in most galaxies apart from the most massive halos proceeds to late times, down to perhaps even the present day (Schawinski *et al.* 2011).

5. Evolution of X-ray Binaries Across Cosmic Time and Energy Feedback at High Redshift.

The possible feedback processes from XRBs at high redshifts ($z \gtrsim 6$) has been the topic of several papers in the last few years. Mirabel *et al.* (2011) considered primordial population-III binaries ($z \gtrsim 6$), and proposed that besides the ultraviolet radiation from massive stars, feedback from accreting BHs in high-mass XRBs (HMXBs) was an additional, important source of heating and re-ionization of the IGM. Justham & Schawinski

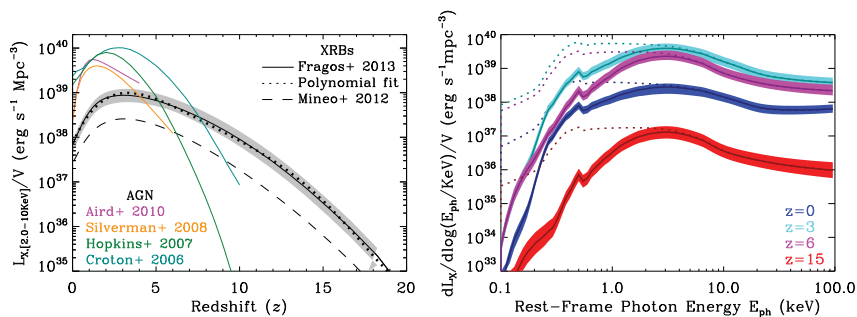


Figure 3. (Left panel) X-ray luminosity per unit co-moving volume in the 2 – 10 KeV band as a function of redshift. The dashed line is derived by convolving the locally measured value of L_X/SFR (Mineo *et al.* 2012) with the SFH of the Universe. For comparison the X-ray luminosity density of AGN in the same energy range is plotted. (Right panel) The SED of the global XRB population at four different redshifts is shown. The solid lines correspond to the mean value of the different models and the shaded area denotes the model uncertainties, assuming in both cases that the interstellar absorption is similar to the Milk Way at all redshifts. With dotted lines we show an estimate of the intrinsic (unabsorbed) SED.

(2012) studied how XRBs inject energy in their local environments before luminous supernovae contribute significantly to feedback. They argue that XRBs can also assist in keeping gas hot long after the last core-collapse SN has exploded. Power *et al.* (2013) explored the ionizing power of HMXBs at high redshifts using simple Monte Carlo modeling for their formation and the Galactic HMXB Cygnus X-1 as a spectral template for their emission in X-rays.

However, we can go now for the first time beyond the order of magnitude calculations or simple rate models for the evolution of XRBs on cosmological timescales. State-of-the-art binary population models provide us with a more physical picture of XRB populations as a function of galaxy properties. This type of detailed modeling has been applied to both starburst and elliptical nearby galaxies, where large populations of individual XRBs are resolved, and detailed ages, star-formation histories, and metallicities are measured (e.g. Fragos *et al.* 2008, 2009, 2010; Luo *et al.* 2012; Tzanavaris *et al.* 2013; Fragos & McClintock 2015; Fragos *et al.* 2015).

Using the *StarTrack* population synthesis code (Belczynski *et al.* 2008), Fragos *et al.* (2013b) performed a large scale population synthesis study that models the X-ray binary populations from the first galaxies of the Universe until today. They used as input to their modeling the Millennium II Cosmological Simulation and the updated semi-analytic galaxy catalog by Guo *et al.* (2011) to self-consistently account for the star-formation history (SFH) and metallicity evolution of the Universe. Their models, which were constrained by the observed X-ray properties of local galaxies, gave predictions about the global scaling of emission from X-ray binary populations with properties such as SFR and stellar mass, and the evolution of these relations with redshift. Although these models were only constrained to observations of the local Universe, they have been shown to be in excellent agreement with X-ray observations of high redshift normal galaxies (e.g. Tremmel *et al.* 2013; Basu-Zych *et al.* 2013b,a).

The emission of X-ray photons in the local Universe is dominated by AGN, whose X-ray flux is approximately an order of magnitude stronger than that coming from XRB populations of normal galaxies. This picture is gradually changing as we move to higher redshifts, with the X-ray luminosity density coming from normal galaxies increasing faster than that from AGN (Fragos *et al.* 2013a). Figure 3 shows that at $z \gtrsim 6 - 8$, XRBs dominate the X-ray luminosity density, since the massive BHs at the centers of galaxies did not have enough time yet to grow and outshine the XRBs.

Using RXTE observations of Galactic neutron star and BH XRBs at different spectral states, and assuming that the interstellar absorption in high redshift galaxies is similar to that in the Milky Way today, we estimate the spectral energy distribution (SED) of a XRB population. We find that the shape of the SED remains approximately constant with redshift, and it is only its normalization that evolves by ~ 4 orders of magnitude (see left panel of Figure 1 and discussion above). The approximately constant SED shape is due to the fact that at all redshifts it is only the brightest BH XRBs in high states that dominate the integrated spectra.

These new studies allow for the first time not only the qualitative but also the quantitative study of the effects of the energy feedback from XRBs in the early Universe.

References

- Agarwal, B., Johnson, J. L., Zackrisson, E., *et al.* 2015, ArXiv e-prints, arXiv:1510.01733
- Basu-Zych, A. R., Lehmer, B. D., Hornschemeier, A. E., *et al.* 2013a, *The Astrophysical Journal*, 774, 152
- . 2013b, *The Astrophysical Journal*, 762, 45
- Belczynski, K., Kalogera, V., Rasio, F. A., *et al.* 2008, *ApJS*, 174, 223
- Cooray, A., Smidt, J., de Bernardis, F., *et al.* 2012, *Nature*, 490, 514
- Feng, Y., Di Matteo, T., Croft, R., *et al.* 2015, *ApJL*, 808, L17
- Feng, Y., Di-Matteo, T., Croft, R. A., *et al.* 2016, *MNRAS*, 455, 2778
- Fiore, F., Puccetti, S., Grazian, A., *et al.* 2012, *A&A*, 537, A16
- Fragos, T., Lehmer, B. D., Naoz, S., Zezas, A., & Basu-Zych, A. 2013a, *ApJL*, 776, L31
- Fragos, T., Linden, T., Kalogera, V., & Sklias, P. 2015, *ApJL*, 802, L5
- Fragos, T., & McClintock, J. E. 2015, *The Astrophysical Journal*, 800, 17
- Fragos, T., Tremmel, M., Rantsiou, E., & Belczynski, K. 2010, *ApJL*, 719, L79
- Fragos, T., Kalogera, V., Belczynski, K., *et al.* 2008, *The Astrophysical Journal*, 683, 346
- Fragos, T., Kalogera, V., Willems, B., *et al.* 2009, *ApJL*, 702, L143
- Fragos, T., Lehmer, B., Tremmel, M., *et al.* 2013b, *The Astrophysical Journal*, 764, 41
- Giallongo, E., Grazian, A., Fiore, F., *et al.* 2015, *A&A*, 578, A83
- Guo, Q., White, S., Boylan-Kolchin, M., *et al.* 2011, *MNRAS*, 413, 101
- Helgason, K., Ricotti, M., & Kashlinsky, A. 2012, *ApJ*, 752, 113
- Justham, S., & Schawinski, K. 2012, *MNRAS*, 423, 1641
- Kashlinsky, A., Arendt, R. G., Ashby, M. L. N., *et al.* 2012, *ApJ*, 753, 63
- Kashlinsky, A., Arendt, R. G., Mather, J., & Moseley, S. H. 2005, *Nature*, 438, 45
- Luo, B., Fabbiano, G., Fragos, T., *et al.* 2012, *The Astrophysical Journal*, 749, 130
- Madau, P., Haardt, F., & Dotti, M. 2014, *ApJL*, 784, L38
- Matsumoto, T., Seo, H. J., Jeong, W.-S., *et al.* 2011, *ApJ*, 742, 124
- Mineo, S., Gilfanov, M., & Sunyaev, R. 2012, *MNRAS*, 419, 2095
- Mirabel, I., Dijkstra, M., Laurent, P., Loeb, A., & Pritchard, J. 2011, *A&A*, 528, A149+
- Mortlock, D. J., Warren, S. J., Venemans, B. P., *et al.* 2011, *Nature*, 474, 616
- Pallottini, A., Ferrara, A., Pacucci, F., *et al.* 2015, *MNRAS*, 453, 2465
- Power, C., James, G., Combet, C., & Wynn, G. 2013, *The Astrophysical Journal*, 764, 76
- Salvaterra, R., Haardt, F., Volonteri, M., & Moretti, A. 2012, *A&A*, 545, L6
- Schawinski, K., Urry, M., Treister, E., *et al.* 2011, *ApJL*, 743, L37
- Sobral, D., Matthee, J., Darvish, B., *et al.* 2015, *ApJ*, 808, 139
- Treister, E., Schawinski, K., Volonteri, M., & Natarajan, P. 2013, *ApJ*, 778, 130
- Tremmel, M., Fragos, T., Lehmer, B. D., *et al.* 2013, *The Astrophysical Journal*, 766, 19
- Tzanavaris, P., Fragos, T., Tremmel, M., *et al.* 2013, *The Astrophysical Journal*, 774, 136
- Volonteri, M., Silk, J., & Dubus, G. 2015, *ApJ*, 804, 148
- Weigel, A. K., Schawinski, K., Treister, E., *et al.* 2015, *MNRAS*, 448, 3167
- Xue, Y. Q., Luo, B., Brandt, W. N., *et al.* 2011, *ApJS*, 195, 10
- Yue, B., Ferrara, A., Salvaterra, R., Xu, Y., & Chen, X. 2013, *MNRAS*, 433, 1556